Inflammation, synovial angiogenesis and chondroid apoptosis in the evolution of type II collagen-induced arthritis

Carlos González[1], Paula Abello[2], Raquel Cepeda[1], Lorena Salazar[3], Octavio Aravena[2], Barbara Pesce[2], Diego Catalán[2], Juan C. Aguillón[2]

[1] Departamento de Patología Animal, Facultad de Ciencias Veterinarias y Pecuarias, Universidad de Chile, Santiago, Chile
[2] Programa Disciplinario de Inmunología, Instituto de Ciencias Biomédicas (ICBM), Facultad de Medicina, Universidad de Chile, Independencia 1027, Santiago, Chile
[3] LS is a fellow from Mecesup-Chile, UCH 0115

Correspondence : J.C. Aguillón, Ph.D
<jaguillo@med.uchile.cl>
Accepted for publication April 25, 2007

ABSTRACT. Using the murine model of type II collagen-induced arthritis (CIA), we studied its evolution over time by histopathological, immunohistochemical and clinical evaluations. The first clinical symptoms appeared 28 days post-inoculation (dpi), with bovine type II collagen, with an average arthritic index of 1.00 ± 0.48 corresponding to erythema of the articulation. The disease progressed, and by 70 dpi showed an average arthritic index of 3.83 ± 0.27 corresponding to edema and maximum deformation, with ankylosis. Computed morphometry demonstrated that, in comparison to controls, the induction of CIA, produces a significant and increasing accumulation of inflammatory cells, fibrosis ($p < 0.0001$) and cartilage destruction ($p = 0.0029$). Likewise, the area of von Willebrand factor (vWF) immunostaining, as an indicator of endothelial proliferation, increased significantly from 28 dpi ($p < 0.0001$), in CIA mice compared to controls. However, the effective synovial vascularization, calculated as the synovial vascular bed area index, significantly increased by 42 dpi ($p = 0.0014$). This indicates that the activation and proliferation of endothelium becomes significant before an effective vascularization area is formed. The apoptosis index was also an earlier indicator of cartilage damage, becoming significant from 28 dpi in comparison to controls ($p < 0.0001$). Finally, it was observed that the increase in the arthritic index showed a strong correlation with the increase in both angiogenesis ($r = 0.95$; $p = 0.0021$) and apoptosis ($r = 0.90$; $p = 0.0015$). In conclusion, a robust correlation between synovial membrane inflammation, angiogenesis and chondrocyte apoptosis, with respect to the increase in the clinical severity of CIA, has been demonstrated by a quantitative computer-assisted immunomorphometric analysis.

Keywords: angiogenesis, apoptosis, arthritis, CIA, morphometric analysis

Rheumatoid arthritis (RA) is characterized by chronic and progressive inflammation of the synovial joints leading to destruction of cartilage and articular bone. In RA, the synovium becomes inflamed and infiltrated by leukocytes. Hyperplasia of synovial cells and inflammatory cells compose the pannus, which is responsible for the local destruction of the joint [1]. RA begins with an abnormal presentation of self-antigens by dendritic cells that leads to activation of self-reactive interleukin (IL)-17-producing CD4+ T lymphocytes, which stimulate macrophages to secrete IL-1, IL-6 and TNF [2-4].

Among several arthritogenic antigens, the participation of endogenous proteins such as type II collagen has been well demonstrated [5]. Moreover, inoculation of the genetically susceptible DBA/1 mouse strain with bovine type II collagen has allowed the development of the type II CIA (CIA) murine model, the most extensively used experimental model of RA [6].

TNF is a great protagonist in RA, inducing apoptosis when binds to its receptor 1 (TNFR1), which presents a high local expression [7]. Under certain conditions, the TNFR1 can activate caspase 8 and induces apoptosis through mechanisms that involve proteins TRADD and FADD [8]. However, studies in synovial fibroblasts have demonstrated that TNF can increase both the transcription of FLIP mRNA and the expression of FLIP protein, a molecule capable of interacting with caspase 8 and FADD, inducing the inhibition of caspase 8 activation, and apoptosis [9]. Likewise, in the cartilage of arthritic articulations, proteins such as p53 and c-myc related to apoptosis, have been detected in chondrocytes with morphological features of apoptosis in a relatively early phase of the destruction of the cartilage, and they also correlated with the degree of degeneration [10].

It has been demonstrated that articular TNF and IL-1 over-expression is crucial both in the generation of the inflammatory process and in the execution of the articular damage [11]. At the synovial membrane level, the hyperplasic process together with a lesser apoptotic activity results in an increase of the synoviocyte number [9]. This creates a hypoxic microenvironment that is believed to trigger the angiogenesis (defined as the development of new capillaries from pre-existing blood vessels) in the synovial membrane, together with the stimuli induced by T lymphocytes, activated macrophages and synovial fibroblasts [12-14]. Through these new capillaries, more in-

doi: 10.1684/ecn.2007.0099

flammatory cells will end up invading the synovial tissue, allowing their proliferation, and perpetuating even more, the articular damage [1].

Formation of new blood vessels within the synovium ensures the development and persistence of the pannus by increasing the supply of nutrients, cytokines and inflammatory cells to the synovial membrane [15]. Vascular endothelial growth factor (VEGF), the main mediator of angiogenesis [15, 16], is found in the synovial fluid and serum of patients with RA [17, 18], and its expression is correlated with disease severity [19, 20]. Compelling evidence that VEGF is involved in synovitis has been obtained from experimental models of RA, using antibodies to VEGF or the soluble VEGF receptor [21-24].

The studies quoted above indicate that both apoptosis and angiogenesis are involved in RA. Thus, chondrocytes have been shown to undergo apoptotic changes in arthritides such as RA and osteoarthritis [25, 26], while angiogenesis leads to leukocyte recruitment and inflammation in the synovium. Furthermore, synovial inflammation itself further potentiates endothelial proliferation, angiogenesis and articular apoptosis. However, although the relationship between synovial inflammation and angiogenesis has been partially assessed [15], the relationship with articular apoptosis has not been defined.

In this work, using the murine model of type II CIA, characterized by the inflammation of multiple articulations, accompanied by synovial hyperplasia, we studied synovial membrane angiogenesis and articular apoptosis in relation to the development of the histopathological lesions occurring in this illness. A quantitative, computer-assisted, immunomorphometric analysis helped to show that both angiogenesis and apoptosis within the joint occur very early during CIA development and that there are correlations between angiogenesis or apoptosis and joint inflammation.

METHODS

Animals

Seven-eight week-old DBA1/lacJ ($H2^q$) mice, obtained from Jackson Laboratories (Bar Harbor, ME, USA), were maintained in accordance with international guidelines for animal care, and protocols were approved by the University of Chile Bioethics Committee.

CIA induction and clinical evaluation of arthritis

As described by Courtenay *et al*. [27], bovine CII protein (Chondrex, Redmond, WA, USA), dissolved in 0.1M acetic acid, was emulsified with Freund's complete adjuvant, and then injected subcutaneously into the base of the tail (100 μg CII/mouse). Immunization was boosted three weeks later by a subcutaneous injection of 100 μg of CII. Three weeks after immunization, mice were clinically examined three times each week. Arthritis severity in the paws was graded according to that described by Yuasa *et al*. [28]: 0 = normal joints, 1 = articular erythema, 2 = swelling with edema and erythema, 3 = severe edema and erythema from articulation to interdigital folds, and 4 = edema and maximum deformation, with ankylosis. The arthritic score of each animal corresponds to the addition of all scores obtained in each one of the four paws, with a maximum of 16 points.

Histopathological analysis

Six mice were sacrificed at 14, 28, 42, 56 and 70 days post-inoculation (dpi) of bovine type II collagen. Simultaneously, three mouse controls, which had been inoculated with saline solution, were also sacrificed. Samples were obtained for histopathology and immunohistochemistry of articular tissue corresponding to the limb that presented the highest arthritic score. Measurements were carried out on each articulation of the selected limb, *i.e.* distal interphalanx articulations, proximal interphalanx, metacarpus or metatarsus phalanges, and intercarpal or intertarsal. The analysis was carried out in 24-hour 10% formalin- fixed tissue samples, which were decalcified in EDTA for six weeks. Paraffin-embedded, 4 μm serial sections were obtained for staining with hematoxylin/eosin and for immunohistochemistry.

Synovial membrane cellular infiltration index (SMCII)

For each selected articulation, images corresponding to the synovial membrane were digitalized with an augmentation of 100x. The SMCII index, expressed in a percentage, was morphometrically calculated as follows: total area corresponding to synovial membrane (μm^2) x 100/total area occupied by cell nuclei (μm^2).

Histopathological damage of articular cartilage

As described by Jou *et al*. [29], the loss of articular cartilage by destruction was graded on a scale of 0-3 (0 = normal cartilage; 1 = slight destruction, with a focal chondrocyte death; 2 = moderate destruction, with multiple foci of chondrocyte death; 3 = severe or total destruction, total chondrocyte death). The final cartilage destruction values were expressed as averages, considering the individual score obtained for all articulations present in the limb that presented the greatest arthritic score.

Degree of fibrosis

Fibrosis severity was diagnosed according to the average number of fibrous layers in five different 100x fields and was classified as: 0 = normal; 1 = slight (1-3 fibrous layers, < 2 foci); 2 = moderate (4-10 fibrous layers, 3-5 foci); 3 = severe (> 10 fibrous layers, > 5 foci).

Immunohistochemistry

In this study, the tissue sections of articulations were previously extended on sylanized glass slides and treated with proteinase K (Dako, USA). After immunostaining, the tissue sections were counterstained with hematoxylin, and mounted with a mounting medium and cover slides, for examination under light microscopy.

Angiogenesis

In order to estimate angiogenesis, the endothelial area was determined by immunostaining with a specific rabbit polyclonal antibody anti-von Willebrand factor. A biotinylated secondary antibody, anti-rabbit IgE was used. The reaction was amplified by a streptovidin/peroxidase conjugate, and revealed with diaminobenzidine as a chromogen sustrate. All reagents used in the procedures described were pur-

chased from Dako (Carpinteria, CA, USA). The endothelial cells were identified after immunostaining by an intense brown colour. The area occupied by these cells was quantitatively analyzed by computer-assisted morphometry and calculated as μm^2/average field. Additionally, the effective synovial vascularization was estimated by calculating the proportional area of synovial membrane corresponding to functional blood vessels represented by those with an expanded lumen with or without erythrocytes inside. This was expressed as a *synovial vascular bed area index* (SVBAI). The SVBAI was calculated as follows: area of synovial membrane x100/area occupied by functional blood vessels.

Apoptosis

The ApopTag®Plus peroxidase *in situ* apoptosis detection kit (Chemicon International INC., Temecula, CA, USA) was used. This kit detects apoptotic cells by specific detection of DNA fragmentation that takes place in the apoptotic process. The articular cartilage apoptotic index was calculated as follows: total nuclear chondrocyte area in cartilage x100/apoptotic nuclear chondrocyte area in cartilage. Nuclear areas in both cases were measured by computer-assisted morphometry.

Computer-assisted morphometric analysis

Images were digitalized with a final resolution of 512 x 480 pixels, using a digital video camera (Cool Snap-Pro CF, Half Cybernetic, USA) mounted in a scientific optical microscope (Nikon Eclipses AND-600) and connected to a computer with software for morphometric analysis (Image Pro-Plus, Media Cybernetics, USA). The measurements of the SMCII (100x field augmentation) and of the immunostained areas for angiogenesis and apoptosis (200x field augmentation) were based on colour detection and expressed in μm^2.

Statistical analysis

For the histopathological study, the values obtained for angiogenesis and apoptosis in the different stages of CIA, were analyzed by variance analysis in a factorial design 2x5'' (ANDEVA), where the two factors to be evaluated were:

1. Induction of the disease factor with two levels (CIA = induced animals; control = animals without induction of the disease).
2. Time factor with five levels (14, 28, 42, 56, and 70 days evaluating for arthritis induction).

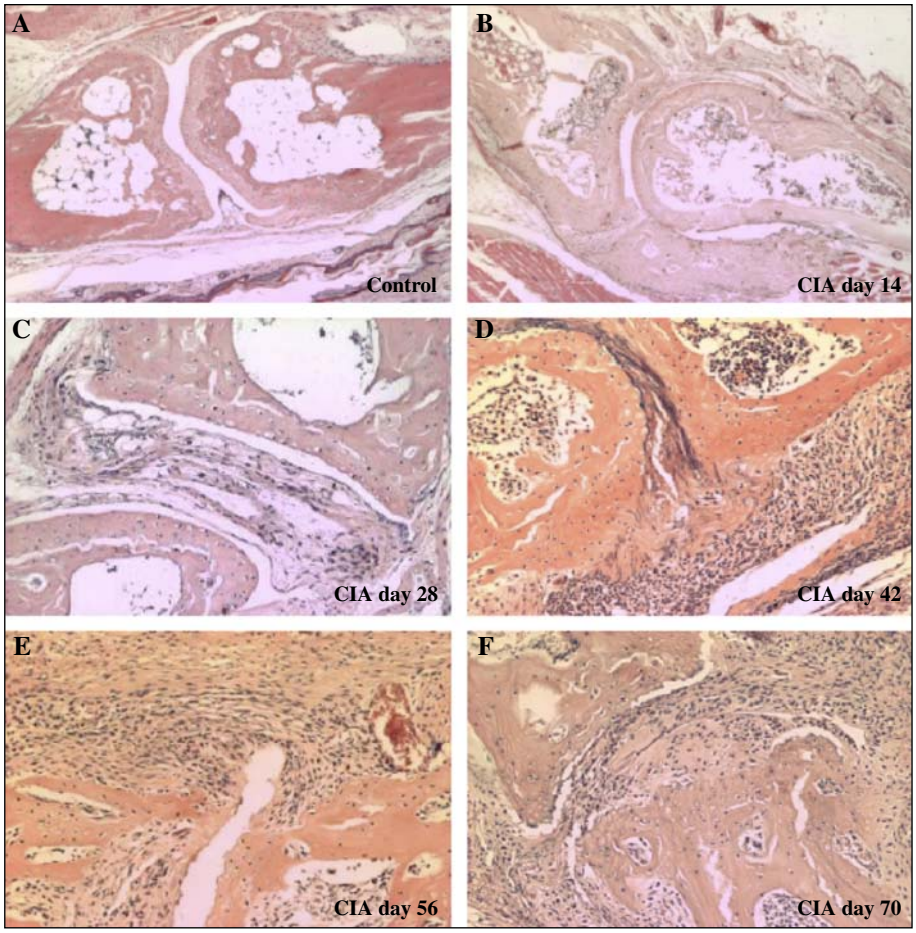

Figure 1

Histopathological analysis of joints after type II CIA was induced in DBA1/lacJ mice. Section of a proximal interphalanx articulation. **A**) Mouse control (40x); **B**) 14 days post-inoculation (dpi) of type II collagen (40x), there are no apparent lesions, and the synovial membrane and the cartilage are still intact. **C**) 28 dpi, initial infiltration of leukocytes especially polymorphonuclear neutrophils in the synovial membrane (100x). **D**) 42 dpi, considerable increase of cellular density is observed in the synovial membrane and the beginning of the pannus formation (40x). **E**) 56 dpi, invasion of the cartilage by the pannus, with initial destruction (100x). **F**) 70 dpi, the pannus has completely destroyed the articular cartilage (100x). The specimens were stained with hematoxylin and eosin.

The variables with a significant effect ($p < 0.05$) were compared with the Tukey's test for multiple ranges [30]. Additionally, the significant differences ($p < 0.05$) of the averages at each time point between the CIA group and controls were analyzed with Sheffé's test [30]. A correlation coefficient was also determined between the variables corresponding to angiogenesis *versus* arthritic index and chondroid apoptosis *versus* arthritic index ($p < 0.05$). The STATA 5.0 software was used for the analysis of relations or associations between the variables [31].

RESULTS

CIA evolution by histopathological analysis

During the development of the disease, an increase in synovial membrane thickness was observed, associated with progressive infiltration by neutrophils, lymphocytes and macrophages at the synovial sub-intima, together with proliferation of cells of the synovial intima, mainly of the fibroblastic type. As the disease became chronic, the formation of fibrous tissue and the proliferation of blood vessels were observed, giving place to the formation of synovial pannus. In *figure 1*, normal control articulation *(figure 1A)*, and the changes observed after the inoculation of bovine type II collagen for CIA induction *(figures 1B* to *1F)* are shown. At 14 dpi, there are no appreciable differences compared to the control *(figure 1B)*; at 28 dpi, the first polymorphonuclear neutrophils are detected, especially in the synovial sub-intima *(figure 1C)*; at 42 dpi, a considerable increase in cellular density of the synovial membrane and formation of the pannus are observed *(figure 1D)*; at 56 dpi, initial destruction of the articular cartilage is observed due to invasion by the pannus *(figure 1E)*; at 70 dpi, complete destruction of the cartilage is shown *(figure 1F)*.

Arthritic index (AI)

Figure 2A shows AIs at 14, 28, 42, 56 and 70 dpi, which increased over time, becoming significantly higher ($p < 0.0001$) from 28 dpi, in comparison to the values obtained for the control group, with an average AI of 1.00 ± 0.81 clinically associated with erythema of the articulation. At 42 dpi, an average AI of 2.33 ± 0.41 was observed, corresponding to edema and erythema of the articulation. At 56 dpi, an average AI of 3.00 ± 0.61 was detected associated with edema and severe erythema, from articulation to the interdigital folds. At 70 dpi, an average AI of 3.83 ± 0.27 was achieved that corresponded to edema and maximum deformation, with ankylosis.

Synovial membrane cellular infiltration index (SMCII)

In *figure 2B*, it can be seen that the SMCII increased over time, while the control group presented no changes. The values obtained for the SMCII in the CIA group were significantly higher than those for the controls starting from 42 dpi (18.34 ± 2.32 *versus* 8.22 ± 0.57) and remaining significant up to 56 dpi (20.73 ± 5.49 *versus*

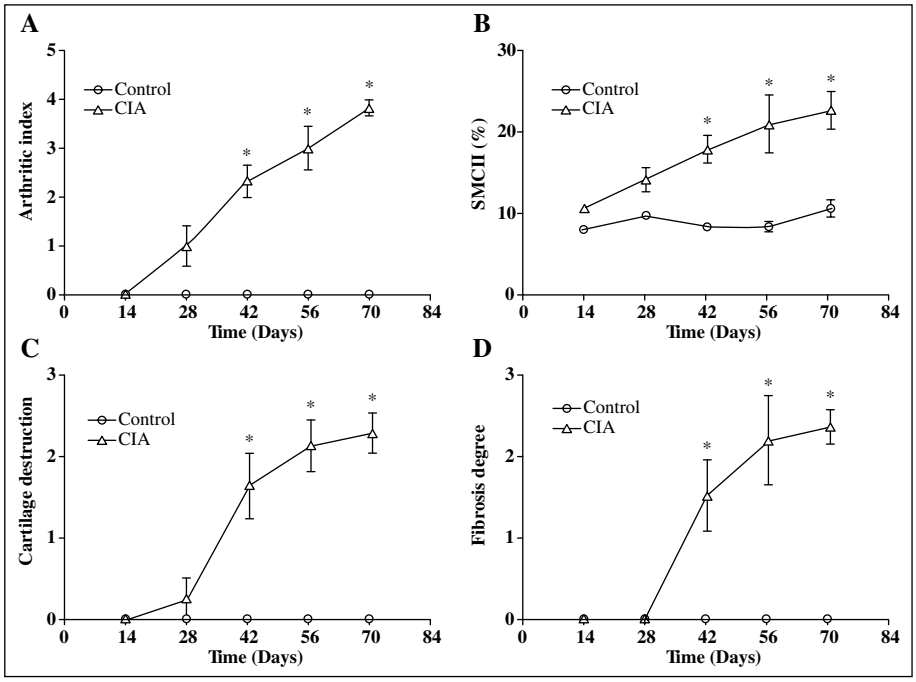

Figure 2

Histopathological evaluation of type II CIA progression over time, at 14, 28, 42, 56, and 70 days post-inoculation (dpi) of bovine collagen for CIA induction. **A**) Arthritic index. **B**) Synovial membrane cellular infiltration index (SMCII) calculated as a ratio between the total area corresponding to synovial membrane (μm^2) and the total area occupied by cell nuclei (μm^2), and expressed as a percentage. **C**) Articular cartilage destruction, which is scored as: 0 = normal; 1 = slight destruction; 2 = moderate destruction; 3 = severe or total destruction. **D**) Degree of fibrosis in the synovial membrane, estimated as follows: 0 = normal; 1 = slight (1-3 fibrous layers, < 2 foci); 2 = moderate (4-10 fibrous layers, 3-5 foci); 3 = severe (> 10 fibrous layers, > 5 foci). The limb that presented the greatest arthritic index was selected in every mouse for all analyses. The results are expressed as average ± S.D. The control group was inoculated with saline solution. The results are expressed as average ± S.D. for each group. Asterisks indicate significant differences ($p < 0.05$) in comparison to controls.

8.30 ± 1.19), and 70 dpi (21.75 ± 3.84 *versus* 10.49 ± 1.79) (p = 0.0019). In the CIA group, the increase of the SMCII was significant both at 56 dpi (20.73 ± 5.49) and at 70 dpi (21.75 ± 3.84), when compared to 14 dpi (10.54 ± 0.52) (p = 0.0019).

Articular cartilage destruction

Figure 2C shows that the degree of destruction of the articular cartilage increased with dpi. However, the animals in the control group, remained at the baseline (0 between 14 and 70 dpi). The cartilage destruction observed in the CIA group was significantly higher than in the control group as from 42 dpi (1.63 ± 0.36 *versus* 0), remaining significant up to 56 dpi (1.75 ± 0.31 *versus* 0), and 70 dpi (2.26 ± 0.28 *versus* 0) (p = 0.0029).

Fibrosis

Figure 2D shows that the degree of fibrosis increased as the disease became chronic, in contrast with the control group that remained in the basal range (0 between 14 and 70 dpi). The values for the degree of fibrosis obtained for the CIA group were significantly higher than those for the control group, starting from 42 dpi (1.50 ± 0.50 *versus* 0), staying significant up to 56 dpi (2.17 ± 0.63 *versus* 0), and 70 dpi (2.33 ± 0.25 *versus* 0) (p = 0.0045). In the CIA group, the increase in the degree of fibrosis was significant both at 56 dpi (2.17 ± 0.33) and at 70 dpi (2.33 ± 0.25), when compared to 14 dpi or to 28 dpi (0) (p < 0.0001).

Angiogenesis in synovial membrane

The immunostaining of von Willebrand endothelial factor (vWF) in synovial membrane was used as an indicator of angiogenesis, and it showed an increase over time in animals induced with the disease, in contrast to the control group *(figures 3A* and *3B)*. Immunostaining was observed in endothelial cells of functional blood vessels of different calibre as well as in endothelial cells of growing angiogenic buds in the sub intima of the synovium. The average area immunostained for vWF in the CIA group was significantly higher than in the control group from 28 dpi (73.01 ± 12.32 *versus* 21.96 ± 3.85) and remained significant at 42 dpi (77.52 ± 21.40 *versus* 19.44 ± 4.17), 56 dpi (91.03 ± 25.97 *versus* 19.66 ± 1.78), and 70 dpi (144.54 ± 21.37 *versus* 22.90 ± 4.90) (p < 0.0001). In the CIA group, the increase in apoptosis was significant at 70 dpi (144.54 ± 21.37) when compared to 14 dpi (29.17 ± 6.97) (p = 0.0154).

In order to determine the effective synovial vascularization, the synovial vascular bed area index (SVBAI) was used. As shown in *figure 3C*, at 42 dpi, the CIA group showed an increase in the SVBAI over time that was significantly higher in comparison to the control group (11.99 ± 1.25 *versus* 4.68 ± 1.55), remaining significant at 56 dpi (15.22 ± 2.48 *versus* 4.38 ± 1.44), and 70 dpi (16.69 ± 2.46 *versus* 5.14 ± 1.11) (p = 0.0014). In the CIA group, the SVBAI over time showed significant differences between 14 dpi and 70 dpi (7.35 ± 1.06 *versus* 16.68 ± 2.12), respectively (p = 0.0178).

Apoptosis in articular cartilage

Fragmentation of DNA was detected immunohistochemically in articular cartilage chondrocytes as an apoptosis indicator. The average articular cartilage apoptotic index in the CIA group increased, together with the number of dpi, while in the control group the values remained at the basal level *(figure 4A)*. As shown in *figure 4B*, an intense degree of chondrocyte apoptosis took place at 70 dpi compared to controls. The statistical analysis showed significant differences between the CIA group and the control group, starting from day 28 dpi (14.99 ± 1.16 *versus* 10.02 ± 0.99), remaining significant up to 42 dpi (20.48 ± 1.33 *versus* 8.18 ± 1.13), 56 dpi (24.20 ± 1.18 *versus* 9.48 ± 0.56), and 70 dpi (28.30 ± 1.25 *versus* 9.62 ± 1.03) (p < 0.0001). In the CIA group, significant differences appeared by14 dpi (9.33 ± 1.14), 42 dpi (20.48 ± 1.33), 56 dpi (24.20 ± 1.18), and 70 dpi (28.30 ± 1.25). A similar situation was observed at 28 dpi (14.99 ± 1.16) *versus* 56 dpi, 28 dpi *versus* 70 dpi, and at 42 dpi *versus* 70 dpi (p < 0.0001).

Relationship between arthritic index, angiogenesis and apoptosis

A correlation index (r) was calculated between both angiogenesis and apoptosis with the index of clinical severity of the disease or arthritic index. As observed in *figure 5A*, the correlation between angiogenesis in the synovial membrane *versus* the arthritic index, shows that they are highly correlated (r = 0.90; p = 0.0021). In a similar way, the apoptotic index in the articular cartilage *versus* the arthritic index were seen to be highly correlated (r = 0.95; p = 0.0015) *(figure 5B)*.

DISCUSSION

Although the results obtained in this study indicate that the leukocyte infiltration into the synovial membrane became significant at 42 dpi, the histopathological analysis revealed that from 14 dpi, polymorphonuclear neutrophils began to appear and accumulated slowly, indicating the beginning of the inflammatory process. It is necessary to consider that their presence, even when discrete, is associated with the liberation of mediators that will lead to progressive leukocyte accumulation and tissue damage that were not significantly demonstrable in this study until 42 dpi, when the fibrosis became significant indicating that the inflammatory process was entering the chronic phase. Furthermore, at the clinical level, as early as 28 dpi, an AI of 1.00 was detected, corresponding to articular erythema. At 42 dpi, the AI was 2.00, corresponding to significant articular edema and erythema.

Thus during disease progression, the synovial membrane thickness increased in the CIA animals, due to both the increase in inflammatory cell infiltration and the increase in fibroblast proliferation. This coincides with the final stage and chronic character of the illness. The synovial membrane cell infiltration index (SMCII) and the degree of fibrosis reached a significant level at 42 dpi, which is in agreement with the results described by De Bandt *et al.* [32]. The workers demonstrated that the blockade of VEGF activity can suppress joint destruction in the K/BxN model of RA while no treated animals developed a more serious cellular pannus from day 32.

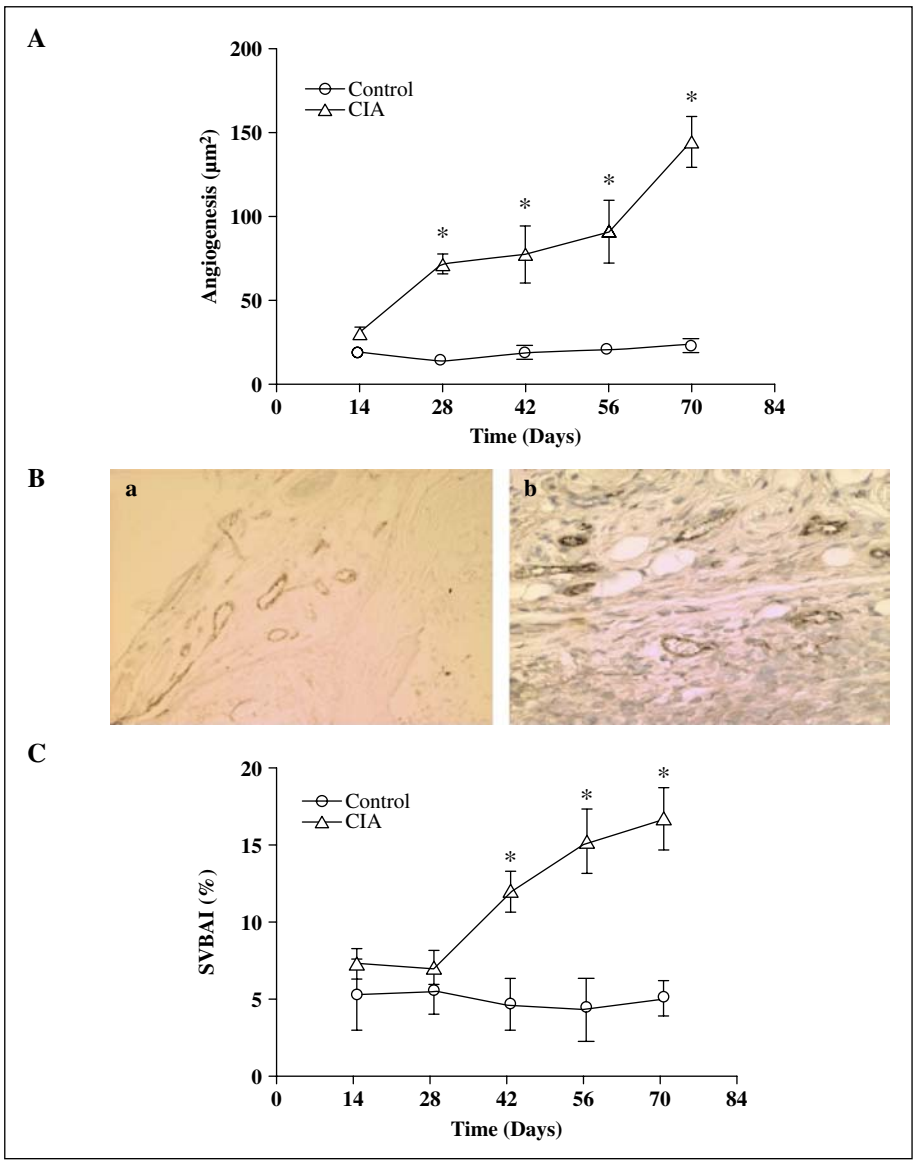

Figure 3

Evaluation of synovial angiogenesis in type II CIA progression over time, at 14, 28, 42, 56, and 70 days post-inoculation (dpi) of bovine collagen for CIA induction. **A**) Average angiogenesis in the synovial membrane was determined by immunohistochemistry. Endothelial area is immunostained with an anti-von Willebrand endothelial factor (vWF) antibody. **B**) photomicrographs of synovial membrane from a control mouse (a), and a CIA mouse, at 70 dpi (b), immunostained for vWF and counterstained with hematoxylin (200x). **C**) synovial vascular bed index, calculated as a ratio between the area of the synovial membrane and the area occupied by functional blood vessels, and expressed as a percentage. The results are expressed as average area (μm^2) ± S.D. or average percentage ± S.D.
Asterisks indicate significant differences ($p < 0.05$) in comparison to controls.

In this study, the inflammation level increased with time, leading towards the formation of a pannus by inflammatory cells, fibrous tissue and newly formed capillary vessels. Likewise, as a consequence of the invasion by this tissue, the articular cartilage was also affected and in most of the articulations it was completely destroyed by 70 dpi. Takeshita *et al*. [33] studied the histopathological changes and IgG deposits in type II collagen-induced rat arthritis. On day 9 after collagen inoculation, although no changes were seen on hematoxylin/eosin (H/E) staining, weak IgG deposits were detected on the surface of synovial lining cells by immunohistochemical staining. On day 11, stratified synovial lining cell proliferation on the surface on the articular capsule, as well as neutrophils, and mononuclear cell infiltration into the synovium, were detected. IgG deposits were densely distributed from the synovial lining cells to the synovium. On day 14, synovial lining cell proliferation and formation of granulation tissue in the synovium were demonstrated by H/E staining, and linear IgG deposition was detected on the surface of the articular cartilage, as well as in the synovial cells. By 18 and 21 dpi, destruction of the articular cartilage and subchondral bone, with neutrophils and increased osteoclasts, and replacement by fibrous tissue were observed on H/E staining.

The immunostaining of vWF as an indicator of angiogenesis, allows us to detect quite early on (14 dpi), the start of angiogenic activity associated with endothelial activation and proliferation. However, the synovial vascular bed area index (SVBAI) was only significant at 42 dpi, in concordance with the increase in leukocyte infiltration in the articular tissue. Similar results have been reported by Lu *et al*. [21] and Clavel *et al*. [15]. These authors, using the same experimental model and measuring vWF and VEGF as angiogenesis indicators, detected high angiogenic activ-

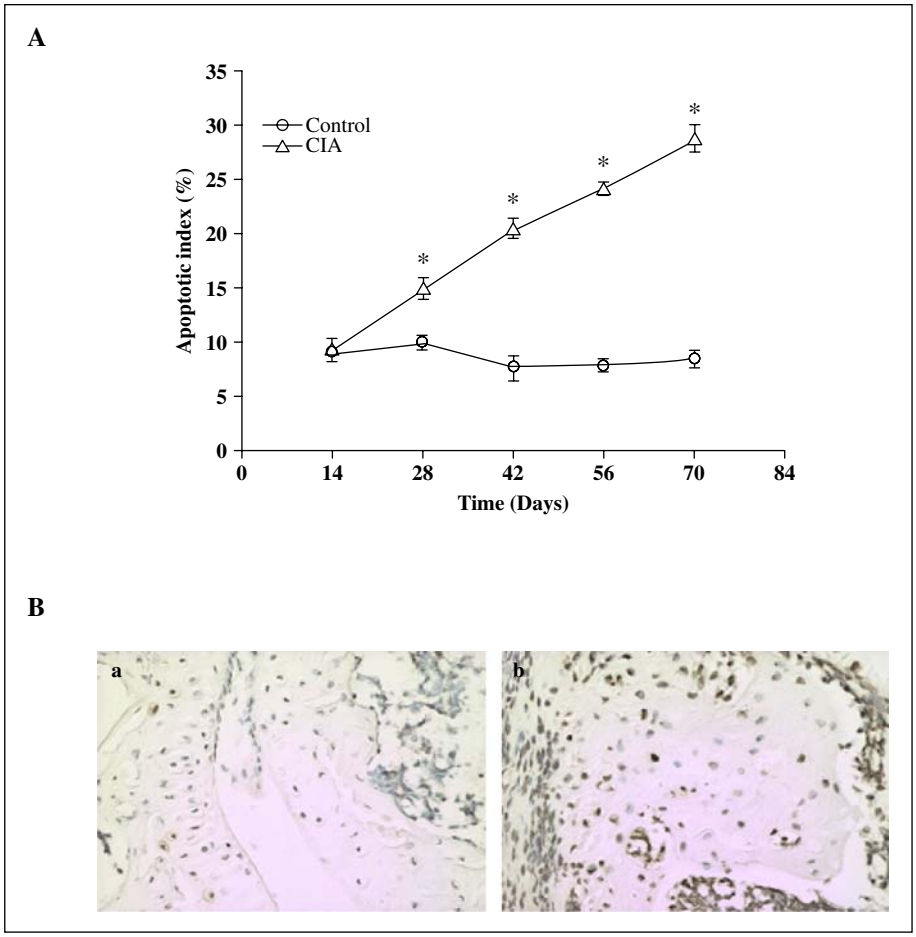

Figure 4

Evaluation of cartilage apoptosis in type II CIA progression over time, at 14, 28, 42, 56, and 70 days post-inoculation (dpi) of bovine collagen for CIA induction. **A**) Apoptotic index in articular cartilage, calculated as the ratio between the nuclear area in cartilage and the apoptotic nuclear area, and expressed as a percentage. Measurements were performed at random in five fields of 200x. **B**) Photomicrographs of articular cartilage from a control mouse (a), and a CIA mouse, at 70 dpi (b). Apoptotic chondrocytes appeared brown in colour by means of ApopTag®/counterstained with hematoxylin (200x). The results are expressed as average percentage ± S.D. for each group. Asterisks indicate significant differences ($p < 0.0001$) in comparison to controls.

ity at 40 dpi, indicating that both vWF and VEGF play a central role in the development of angiogenesis as a response to cytokines such as IL-1, TNF and IL-8. The increase in cells in the arthritic synovium creates a hypoxic microenvironment that induces the generation of free radicals and nitric oxide (NO), which are able to stimulate VEGF production. Furthermore, NO is responsible for inducing mutations on the p53 gene leading to diminished apoptosis of the synovial fibroblasts, contributing to increase synovial membrane thickness [34]. In addition, Schmitt-Sody *et al*. [35] have also reported that the immunostaining for vWF, in samples of knees from an antigen-induced murine arthritis experimental model, demonstrated high angiogenic activity and a high clinical index of severity by day 8.

Immunohistochemisty revealed that at 14 dpi, it was possible to observe manifestations of angiogenic activity in the form of blood vessel buds, becoming significant after 28 dpi. However, the increase in effective vascular tissue in the synovial membrane, expressed as the synovial vascular bed area in relation to the total tissue area, became significant only after 42 dpi. The same was observed for leukocyte accumulation.

In a similar way, destruction of the articular cartilage became significant after 42 dpi, which is in agreement with results obtained by Larsson *et al*. [36] who also carried out a study of cartilage destruction, detecting cartilage oligomeric matrix protein in mice serum. Their experimental model involved 30 days of study after collagen inoculation, and by this time point they found the highest serum concentration of these proteins associated with cartilage destruction.

It is well established that the immunostaining of chondrocyte apoptosis constitutes an earlier indicator of damage. The present study revealed that at 28 dpi, it is possible to observe a significant increase in apoptotic activity that continues to increase up to 70 dpi, indicating that apoptotic index of the articular cartilage increases as the disease progresses. These results agree with those described by Van't Hof *et al*. [34], who carried out *in vitro* studies of human synovial tissue and articular cartilage, and with those of Tak *et al*. [37], who carried out their studies in an antigen-induced arthritis model. It is worth drawing attention to the fact that in an inflammatory atmosphere the production of NO, a well recognized pro-apoptotic agent, is highly increased, and becomes one of the causative agents of articular cartilage destruction [34].

The conventional histopathology and immunohistochemistry allowed detection of changes that, although discrete, are clear indicators of the establishment of the inflamma-

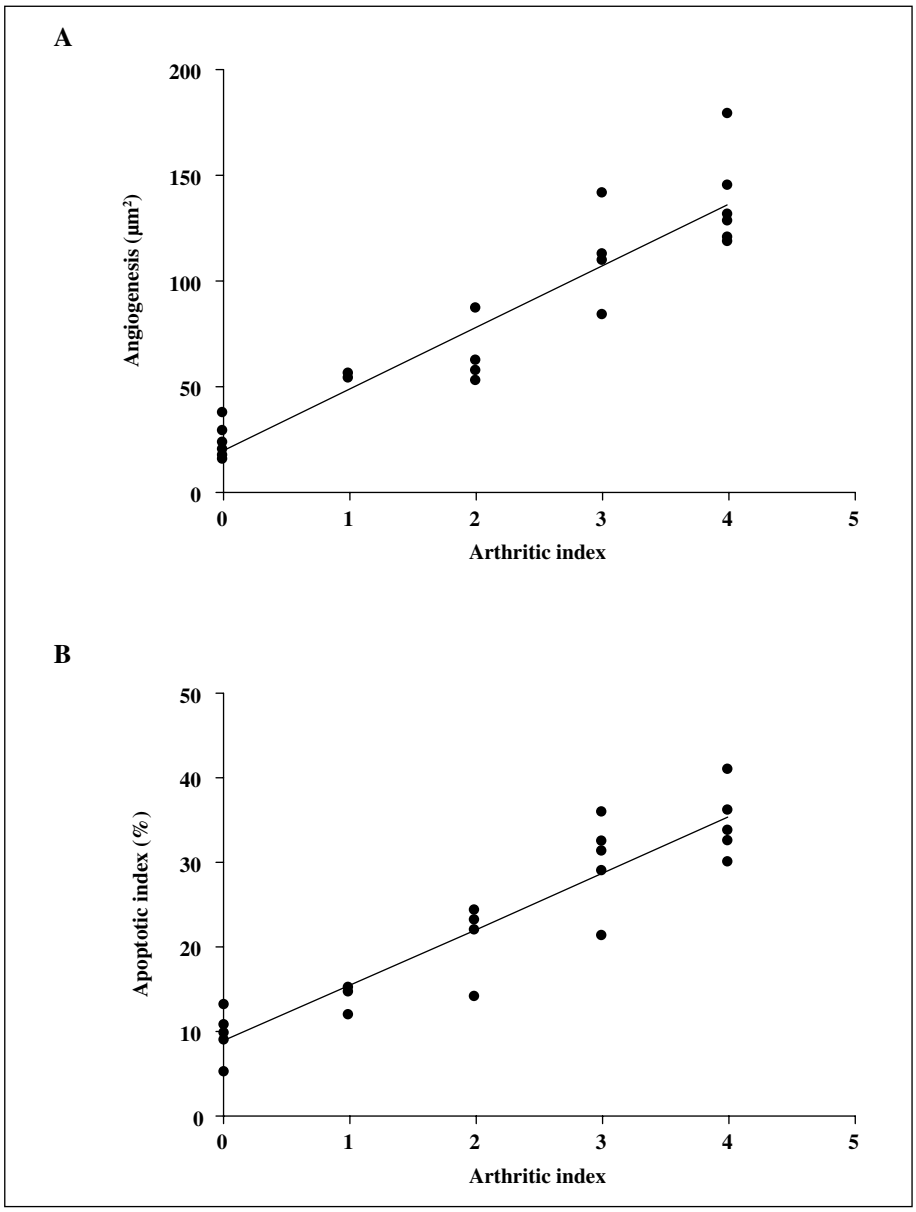

Figure 5

A) Relationship between synovial angiogenesis and the arthritic index in type II CIA (r = 0.90; p = 0.0021). **B**) relationship between articular cartilage apoptosis and the arthritic index (r = 0.95; p = 0.0015). In both cases, the parameters are highly correlated.

tory process. These changes include the appearance of polymorphonuclear neutrophils in the synovial membrane, endothelial proliferation with development of angiogenic buds, and the increase in the chondrocyte apoptotic activity that happens earlier.

The apoptotic index was an earlier indicator of damage in the articular cartilage, becoming significant in comparison to its control from 28 dpi. While immunostaining of vWF was an earlier indicator of endothelial activation and the beginning of the angiogenic activity with endothelial cell proliferation and formation of angiogenic buds, it also became significant by 28 dpi. In this period, at the clinical level, the first manifestations of the disease appeared with an average arthritic index close to 1.

Furthermore, our study shows a strong correlation between angiogenesis and clinical severity of the disease or arthritic index. These results suggest that angiogenesis contributes to joint damage by increasing the vascularity of the inflammatory pannus, thereby supporting its growth and facilitating inflammatory cell infiltration. In addition, we describe a robust correlation between apoptosis and the arthritic index. Thus, our data propose that in CIA mice, apoptotic chondrocytes significantly increase with disease progression. Chondrocyte apoptosis may destroy the cartilage restoration process, eventually resulting in bone-cartilage deformation [26, 38, 39]. Spears *et al*. [40] demonstrated an increase in apoptotic cells in acute arthritis induced by direct injection of Freund's complete adjuvant in rats; they detected an increased number of TUNEL positive cells and the activation of caspase-3 and -8 in cultured tissue.

Finally, these results may become useful as a reference point for future investigations that may include the application of possible therapies focused on regulating apoptosis and the formation of new blood vessels, as these events are crucial in the progress and maintenance of the disease.

Acknowledgements. *We thank Ms. Nancy Fabres and Ms. Juana Orellana for their excellent technical assistance and Mr. Miguel Sepúlveda for histologic work. The study was supported by Fondecyt-Chile (104-0860), Millennium Nucleus on Immunology and Immunotherapy-Chile (P04/030-F) and FONDEF-Chile (D03I1055).*

REFERENCES

1. Paleolog EM. Angiogenesis in rheumatoid arthritis. *Arthritis Res* 2002; 4: S81.
2. Weyand C, Goronzy J. The molecular basis of rheumatoid arthritis. *J Mol Med* 1997; 75: 772.
3. Lee DM, Weinblatt ME. Rheumatoid arthritis. *Lancet* 2001; 358: 903.
4. Feldman M, Brennan FM, Maini RN. Role of cytokines in rheumatoid arthritis. *Annu Rev Immunol* 1996; 14: 397.
5. Rosloniec EF, Brand DD, Myers LK, *et al.* An HLA-DR1 transgene confers susceptibility to collagen-induced arthritis elicited with human type II collagen. *J Exp Med* 1997; 185: 1113.
6. Brand DD, Kang AH, Rosloniec EF. Immunopathogenesis of collagen arthritis. *Springer Semin Immunopathol* 2003; 25: 3.
7. Deleuran BW, Chu CQ, Field M, Brennan FM, Mitchel T, Feldman M. Localization of tumor necrosis factor receptors in the synovial tissue and cartilage – pannus junction in patients with rheumatoid arthritis: Implications for local actions of tumor necrosis factor α. *Arthritis Rheum* 1998; 32: 1170.
8. Hsu H, Xiong J, Goeddel DV. The TNF receptor 1 associated protein TRADD signals cell death and NF-κB activation. *Cell* 1995; 81: 495.
9. Bai S, Liu H, Chen KH, Eksarko P, Perlman H, Moore TL, Pope RM. NF-κB- regulated expression of cellular FLIP protects rheumatoid arthritis synovial fibroblasts from tumor necrosis factor α-mediated apoptosis. *Arthritis Rheum* 2004; 50: 3844.
10. Yatsugi N, Tzukazaki T, Osaki N, Koji T, Yamashita S, Shindo H. Apoptosis of articular chondrocytes in rheumatoid arthritis and osteoarthritis: Correlation of apoptosis with degree of cartilage destruction and expression of apoptosis-related protein p53 and c-myc. *J Orthop Sci* 2000; 5: 150.
11. Macnaul KL, Hutchinson NI, Parsons JN, Bayne EK, Tocci MJ. Analysis of IL-1 and TNF-alpha gene expression in human rheumatoid synoviocytes and normal monocytes by in situ hybridization. *J Immunol* 1990; 145: 4154.
12. Colville-Nash PR, Scout DL. Angiogenesis and rheumatoid arthritis: Pathogenic and therapeutic implications. *Ann Rheum Dis* 1992; 51: 919.
13. Walsh DA. Angiogenesis and arthritis. *Rheumatol* 1999; 38: 103.
14. Koch AE. Angiogenesis as target in rheumatoid arthritis. *Ann Rheum Dis* 2003; 62: 60.
15. Clavel G, Valvason C, Yamaoka K, *et al.* Relationship between angiogenesis and inflammation in experimental arthritis. *Eur Cytokine Netw* 2006; 17: 1.
16. Clavel G, Bessis N, Boissier MC. Recent data on the role for angiogenesis in rheumatoid arthritis. *Joint Bone Spine* 2003; 70: 321.
17. Paleolog EM, Young S, Stark AC, *et al.* Modulation of angiogenic vascular endothelial growth factor by tumor necrosis factor-a and interleukin-1 in rheumatoid arthritis. *Arthritis Rheum* 1998; 41: 1258.
18. Nagashima M, Asano G, Yoshino S. Imbalance in production between vascular endothelial growth factor and endostatin in patients with rheumatoid arthritis. *J Rheumatol* 2000; 27: 2339.
19. Fava RA, Olsen NJ, Spencer-Green G, *et al.* Vascular permeability factor/endothelial growth factor (VPF/VEGF): accumulation and expression in human synovial fluids and rheumatoid synovial tissue. *J Exp Med* 1994; 180: 341.
20. Maeno N, Takei S, Imanaka H, *et al.* Increased circulating vascular endothelial growth factor is correlated with disease activity in polyarticular juvenile rheumatoid arthritis. *J Rheumatol* 1999; 10: 2244.
21. Lu J, Kasama T, Kobayashi K, *et al.* Vascular endothelial growth factor expression and regulation of murine collagen-induced arthritis. *J Immunol* 2000; 164: 5922.
22. Sone H, Kawakami Y, Sakauchi M, *et al.* Neutralization of vascular endothelial growth factor prevents collagen-induced arthritis and ameliorates established disease in mice. *Biochem Biophys Res Commun* 2001; 281: 562.
23. Sekimoto T, Hamada K, Oike Y, *et al.* Effect of direct angiogenesis inhibition in rheumatoid arthritis using a soluble vascular endothelial growth factor receptor 1 chimeric protein. *J Rheumatol* 2002; 29: 240.
24. Miotla J, Maciewicz R, Kendrew J, *et al.* Treatment with soluble VEGF receptor reduces disease severity in murine collagen-induced arthritis. *Lab Invest* 2000; 80: 1195.
25. Hashimoto S, Ochs RL, Rosen F, *et al.* Chondrocyte derived apoptotic bodies and calcification of articular cartilage. *Proc Natl Acad Sci USA* 1998; 95: 3094.
26. Blanco FJ, Guitian R, Vazquez-Martul E, *et al.* Osteoarthritis chondrocytes die by apoptosis. A possible pathway for osteoarthritis pathology. *Artritis Rheum* 1998; 41: 284.
27. Courtenay JS, Dallman MJ, Dayan AD, *et al.* Immunisation against heterologous type II collagen induces arthritis in mice. *Nature* 1980; 283: 666.
28. Yuasa T, Kubo S, Yoshino T, *et al.* Deletion of Fcgamma receptor IIb renders H-2(b) mice susceptible to collagen-induced arthritis. *J Exp Med* 1999; 189: 187.
29. Jou IM, Shiau AL, Chen SY, *et al.* Thrombospondin 1 as an effective gene therapeutic strategy in collagen induced arthritis. *Arthritis Rheum* 2005; 52: 339.
30. Steel RGD, Torrie JH. *Principles and procedures of statistics: A biometral approach*. Mc Graw-Hill, New York: México, 1980.
31. StataCorp. *STATA Statistical Software: Release 5.0*. College Station, TX: Stata Corporation. U.S.A., 1997.
32. De Bandt M, Ben Mahdi MH, Ollivier V, *et al.* Blockade of vascular endothelial growth factor receptor I (VEGF-RI), but not VEGF-RII, suppresses joint destruction in the K/BxN model of rheumatoid arthritis. *J Immunol* 2003; 171: 4853.
33. Takeshita M, Hinoue H, Furukawa O, *et al.* Initial arthritic lesions induced by immunization with type II collagen in Lewis rats. *Exp Anim* 1995; 44: 63.
34. Van't Hof RJ, Hocking L, Wright PK, *et al.* Nitric oxide is a mediator of apoptosis in the rheumatoid joint. *Rheumatol* 2000; 39: 1004.
35. Schmitt-Sody M, Landes J, Zysk SP, *et al.* Quantitative assessment of angiogenesis in murine antigen-induced arthritis by intravital fluorescence microscopy. *J Vasc Res* 2003; 40: 460.
36. Larsson E, Muèssener A, Heinegaê D, *et al.* Increased serum levels of cartilage oligomeric matrix protein and bone sialoprotein in rats with collagen arthritis. *Rheumatol* 1997; 36: 1258.
37. Tak PP, Klapwijk MS, Broersen SF, *et al.* Apoptosis and p53 expression in rat adjuvant arthritis. *Arthritis Res* 2000; 2: 229.
38. Kim HA, Lee YJ, Seong SH, *et al.* Apoptotic chondrocyte death in human osteoarthritis. *J Rheumatol* 2000; 27: 455.
39. Lots M, Hashimoto S, Kühn K. Mechanisms of chondrocyte apoptosis. *Osteoarthritis Cartilage* 1999; 7: 389.
40. Spears R, Oakes R, Bellinger LL, *et al.* Tumor necrosis factor-alpha and apoptosis in the rat temporomandibular joint. *Arch Oral Biol* 2003; 48: 825.